Applied Catalysis B: Environmental 127 (2012) 273–280

Contents lists available at SciVerse ScienceDirect

Applied Catalysis B: Environmental

journal homepage: www.elsevier.com/locate/apcatb

Rational direct synthesis methodology of very active and hydrothermally stable Cu-SAPO-34 molecular sieves for the SCR of NO_x

Raquel Martínez-Franco[a], Manuel Moliner[a,*], Cristina Franch[a], Arkady Kustov[b], Avelino Corma[a,**]

[a] Instituto de Tecnología Química (UPV-CSIC), Universidad Politécnica de Valencia, Consejo Superior de Investigaciones Científicas, Valencia 46022, Spain
[b] Haldor Topsøe A/S, Nymøllevej 55, DK-2800 Lyngby, Denmark

ARTICLE INFO

Article history:
Received 26 June 2012
Received in revised form 3 August 2012
Accepted 28 August 2012
Available online 5 September 2012

Keywords:
One-pot synthesis
Silicoaluminophosphate
SAPO-34
Selective catalytic reduction (SCR)
Nitrogen oxides (NO_x)

ABSTRACT

A one-pot direct synthesis of Cu-SAPO-34 has been achieved that allows more than 90% yield in the material synthesis. By this method it is easy to control the Cu-loading in the Cu-SAPO-34. It is presented that a maximum in hydrothermal stability with very high activity for NO_x SCR with NH_3 is obtained for an optimum Cu loading.

1. Introduction

Nitrogen oxides (NO_x), involving nitric oxide (NO), nitrogen dioxide (NO_2) and nitrous oxide (N_2O) are major air pollutants [1]. NO_x is generated primary by the combustion of fossil fuels, both in transportation and industrial processes. However, transports, and especially those working with diesel engines, are the main sources of NO_x emissions [2]. Selective catalytic reduction (SCR) of NO_x by ammonia has become the most used emission control [3], and catalysts based on vanadia are in commercial use since 2005 for diesel vehicles [4]. However, vanadia catalysts suffer some serious drawbacks, as oxidation of SO_2 to SO_3 (which would react with H_2O resulting in H_2SO_4), and low activity and selectivity at high temperatures due to the sintering of vanadia species [5].

The discovery of copper-exchanged zeolites as active and stable catalysts for the SCR of NO_x by Iwamoto et al. introduced an attractive alternative to vanadia-based materials [6]. Several metal-exchanged molecular sieves, primary medium and large pore zeolites, have been reported in the last two decades for the SCR of NO_x [7]. Unfortunately, those materials present low hydrothermal stability when reacting under harsh conditions (presence of steam at high temperatures). Recently, BASF researchers have described that copper-containing small-pore chabazite zeolite shows much better hydrothermal stability than large pore zeolites (Cu-Beta or Cu-Y) [8]. This description has revived the industrial interest in metal-containing molecular sieves for NO_x abatement [9]. In this sense, Fickel and Lobo [10] have reported that the higher hydrothermal stability and better catalytic behavior of Cu-CHA for SCR of NO_x is due to the localization of copper atoms coordinated to the double six-membered rings units (D6-MR) present in the large cavities of chabazite structure.

Conventionally, those metal-containing molecular sieves are obtained by post-synthesis ion-exchange procedures. Indeed, several steps, such as hydrothermal synthesis of the molecular sieves, calcination, metal ion exchange, and calcination are required to get the final metal-containing molecular sieves.

Recently, Xiao et al. [11] have nicely reported the direct preparation of Cu-SSZ-13 zeolite (SSZ-13 is the silicoaluminate form of the CHA structure) by using a low-cost copper–amine complex (Cu^{2+} with tetraethylenepentamine, Cu-TEPA) as an efficient template. This methodology allowed the direct introduction of extra-framework copper species in the CHA cages, revealing promising results in SCR of NO_x reaction. Despite the remarkable impact that this discovery could have on the NO_x field, the materials reported in this manuscript suffer from important drawbacks. SSZ-13 syntheses with several Si/Al ratios (5, 7.5, 12.5, and 17.5) were attempted, but the final Si/Al ratios into the solids were much lower (4.1, 4.3, 5.3, and 7.5, respectively). These values clearly indicate that large part of the initially introduced silicon species remained in solution when the Si/Al ratio was increased, notoriously affecting

* Corresponding author.
** Corresponding author. Tel.: +34 96 3877800; fax: +34 96 3877809.
E-mail addresses: mmoliner@itq.upv.es (M. Moliner), acorma@itq.upv.es (A. Corma).

0926-3373/$ – see front matter © 2012 Elsevier B.V. All rights reserved.
http://dx.doi.org/10.1016/j.apcatb.2012.08.034

to the SSZ-13 yield. Moreover, the desired industrial catalysts for the SCR of NO_x must show high hydrothermal stability due to the reaction conditions, i.e. high temperature and presence of steam. It is well known that zeolites with low Si/Al ratio (less than 10) suffer severe dealumination processes in presence of steam at high temperature [12]. In fact, the SCR of NO_x experiment described by Xiao was performed on the sample with Si/Al ratio of 4.1 under mild conditions (low space velocity), and the stability of the synthesized samples under hydrothermal treatments was not studied. Furthermore, the different Cu-SSZ-13 examples reported by Xiao et al. show similar Cu loadings (Cu/Si = 0.09–0.10), indicating that the amount of Cu on SSZ-13 samples cannot be easily varied in a controlled manner.

In addition to SSZ-13, the chabazite molecular sieve can be synthesized as silicoaluminophosphate form, SAPO-34 [13]. Cu-exchanged SAPO-34 has also been shown as a very stable and active material for SCR of NO_x [14]. In the last years, some groups have attempted the direct preparation of Cu-SAPO-34 in order to achieve an inexpensive and more efficient synthetic route for this metal-substituted material [15]. In those cases morfoline and copper oxide were used as organic structure directing agent (OSDA) and copper source, respectively. Those crystalline Cu-SAPO-34 materials show very low Cu contents [Cu/(Al + P) = 0.02], and samples with higher Cu loadings direct into amorphous materials, low solid yields (lower than 70% of initial sources), and mixture of metal in framework positions and extra-framework cationic positions [15c]. During the preparation of the present manuscript, a very interesting paper studying the effect of the synthesis approach (cation exchange, chemical vapor deposition and direct synthesis) on the nature of the Cu active site, and therefore, on the SCR of NO_x activity, has been published [16]. In that work, the authors showed the direct synthesis preparation of Cu-SAPO-34 material by using a combination of templates, such as the Cu^{2+}-triethylenetetramine complex and tetraethylammonium cations, obtaining interesting catalytic results for the SCR of NO_x. Those experiments were performed in absence of steam, and moreover, the catalyst stability tests against severe ageing treatments were not carried out.

Herein, we will show a very detailed and rationalized "one-pot" Cu-SAPO-34 preparation, from the use of a Cu-complex (Cu^{2+} with tetraethylenepentamine, Cu-TEPA) as the unique template, to the cooperative and fundamental role of a small organic molecule (as diethylamine, DEA) acting as co-template. Following this rationalized direct synthesis methodology, the Cu-loading in extra-framework positions into the material can be easily controlled, and the final solid yields obtained are very high (larger than 90% of expected solids from initial precursors). Those Cu-SAPO-34 samples are extremely active and hydrothermally stable when tested in the SCR of NO_x reaction under very severe reaction conditions (very high space velocity, and presence of steam at very high temperatures). The combination of the direct synthesis of Cu-SAPO-34 together with hydrothermal stability and excellent catalytic results obtained for the SCR of NO_x introduces new opportunities for the industrial use of this type of material.

2. Experimental

2.1. Synthesis

2.1.1. Direct syntheses of Cu-SAPO-34 materials

In a general procedure for the Cu-SAPO-34 preparation, the Cu-complex was firstly prepared by mixing a 20 wt% of an aqueous solution of copper (II) sulfate (98 wt%, Alfa) with the tetraethylenepentamine (TEPA, 99 wt%, Aldrich). This mixture was stirred for 2 h until complete dissolution. Secondly, distilled water and phosphoric acid (85% wt, Aldrich) were added and stirred during 5 min. Third, alumina (75 wt%, Condea) and silica (Ludox AS40 40 wt%, Aldrich) sources were introduced in the gel mixture. Finally, diethylamine (DEA, 99 wt%, Aldrich) and SAPO-34 seeds (5 wt% of expected final yield), if required, were added in the gel, and the mixture was stirred during 30 min. The resulting gel was transferred to an autoclave with a Teflon liner, and heated at 150 °C under static conditions during the required time (see experimental conditions for each sample in Tables 1, 3 and 4). Crystalline products were filtered and washed with abundant water, and dried at 100 °C overnight. The samples were calcined at 550 °C in air to properly remove the occluded organic species.

Table 1
Experimental design for the direct hydrothermal synthesis of silicoaluminophosphates by using different amounts of Cu-complex as OSDA (T = 150 °C static conditions, t = 7 days).

Variable	Values
Cu-TEPA/(Al + P)	0.2, 0.5
H_2O/(Al + P)	10, 30, 50
P/Al	0.8, 0.9
[Si/(Al + P)]	[0.2, 0.1, respectively]

2.1.2. SAPO-34 synthesis for post-synthesis Cu-exchange

SAPO-34 was synthesized following the procedure described in the literature [17]. The molar gel composition was: 2 DEA:0.6 SiO_2:1 Al_2O_3:0.8 P_2O_5:50 H_2O, keeping the mixture autoclaved at 200 °C during 72 h. The resulting product was filtered and washed with distilled water, and dried at 100 °C overnight. The sample was calcined at 550 °C in air to remove the occluded organic species.

In order to perform the Cu ion exchange on this SAPO-34 material, the calcined sample was first washed with $NaNO_3$ (0.04 M), and afterwards, the sample was exchanged at room temperature with a $Cu(CH_3CO_2)_2$ solution (solid/liquid ratio of 10 g/L). Finally, the sample was filtered and washed with distilled water, and calcined at 550 °C for 4 h.

2.2. Characterization

X-ray diffraction (XRD) measurements were performed on a multisample Philips X'Pert diffractometer equipped with a graphite monochromator, operating at 40 kV and 45 mA, and using Cu Kα radiation (λ = 0.1542 nm).

The chemical analyses were carried out in a Varian 715-ES ICP-Optical Emission spectrometer, after solid dissolution in HNO_3/HCl/HF aqueous solution. The organic content of as-made materials was determined by elemental analysis performed on a SCHN FISONS element analyzer. Thermogravimetrical analysis was evaluated using a Mettler Toledo thermo-balance.

Textural properties were determined by N_2 adsorption–desorption isotherms measured on a Micromeritics ASAP 2020 at 77 K.

The morphology of the samples was studied by scanning electron microscopy (SEM) using a JEOL JSM-6300 microscope.

The NMR spectra were recorded at room temperature on a Bruker AV 400 spectrometer MAS. ^{29}Si NMR spectra were recorded with a spinning rate of 5 kHz at 79.459 MHz with a 55° pulse length of 3.5 μs and repetition time of 180 s. ^{27}Al MAS NMR spectra were recorded at 104.2 MHz with a spinning rate of 10 kHz and a 9° pulse length of 0.5 μs with a 1 s repetition time. Solid-state ^{31}P NMR spectra were recorded at 161.9 MHz with a spinning rate of 10 kHz, a $\pi/2$ pulse of 5 μs with 20 s repetition time.

^{29}Si, ^{27}Al and ^{31}P chemical shifts were referred to tetramethylsilane, $Al^{3+}(H_2O)_6$, and 85% H_3PO_4, respectively.

2.3. Catalytic experiments

The activity of the samples for the selective catalytic reduction of NO_x using NH_3 as reductor was tested in a fixed bed, quartz tubular reactor of 2.2 cm of diameter and 53 cm of length. The total gas flow was fixed at 300 mL/min, containing 500 ppm of NO, 530 ppm of NH_3, 7% of O_2, and 5% of H_2O. The catalyst (40 mg) was introduced in the reactor, heated up to 550 °C and maintained at this temperature for 1 h under nitrogen flow. After that the desired reaction temperature was set (170–550 °C) and the reaction feed admitted. The NO_x present in the outlet gases from the reactor were analyzed continuously by means of a chemiluminiscence detector (Thermo 62C).

2.4. Steaming procedures

The hydrothermal stability of metal-containing molecular sieves was studied by steaming with water (2.2 mL/min) at 600 °C or 750 °C during 13 h in an oven.

3. Results

3.1. Direct synthesis of Cu-SAPO-34 using Cu-TEPA as the unique organic template

We have first studied the use of the Cu-complex formed by Cu^{2+} with tetraethylenepentamine (TEPA) in the typical synthesis conditions of SAPO-34 as the unique organic template. Two different molar ratios of Cu-complex, three of water, and two P/Al ratios [and consequently two Si/(P + Al)] were screened in order to synthesize Cu-SAPO-34 by a "one-pot" methodology. The experimental design performed is summarized in Table 1.

As it can be seen in Fig. 1, Cu-SAPO-34 materials were only achieved when a large amount of complex was introduced in the synthesis media [Cu-TEPA/(Al + P) = 0.5]. If the Cu-complex content was reduced [Cu-TEPA/(Al + P) = 0.2], amorphous materials were obtained. Fig. 2 shows the XRD patterns of the SAPO34-1 (as referred in Fig. 1) in as-prepared form and after calcination in air at 550 °C. The XRD patterns confirm the CHA structure of those samples, and also reveal their stability after regular calcinations in air at 550 °C. The other synthesized Cu-SAPO-34 samples in the present study (see Fig. 1), show similar XRD patterns.

Chemical analyses were performed on synthesized Cu-SAPO-34 materials in order to study their real Cu-content. As seen in Table 2, SAPO34-1 and SAPO34-4 samples show higher Cu-contents [Cu/(Al + P) = 0.21] than the other SAPO-34 samples [Cu/(Al + P) = 0.13–0.14]. It seems that under these synthesis conditions, the gel dilution plays an important role in the Cu-loading, achieving larger Cu-loadings for lower water content

				P/Al = 0,9 Si/(Al+P) = 0,1	P/Al = 0,8 Si/(Al+P) = 0,2
H_2O/(Al+P)	10	Cu-TEPA/(Al+P)	0,2		
			0,5	SAPO34-1	SAPO34-4
	30	Cu-TEPA/(Al+P)	0,2		
			0,5	SAPO34-2	SAPO34-5
	50	Cu-TEPA/(Al+P)	0,2		
			0,5	SAPO34-3	SAPO34-6

Amorphous
SAPO-34

Fig. 1. Phases obtained for the direct hydrothermal synthesis of silicoaluminophosphates by using Cu-TEPA as the unique organic template.

Table 2
Chemical and elemental analyses of Cu-SAPO-34 samples achieved by using Cu-TEPA as OSDA.

Sample	Si/(Al + P)	Cu/(Al + P)	$(C/N)_{real}$	$(C/N)_{teor}$
SAPO34-1	0.27	0.21	1.6	1.6
SAPO34-2	0.18	0.14	1.6	1.6
SAPO34-3	0.17	0.14	1.6	1.6
SAPO34-4	0.23	0.21	1.6	1.6
SAPO34-5	0.22	0.13	1.6	1.6
SAPO34-6	0.23	0.13	1.6	1.6
SAPO34-Exc	0.15	0.07	–	–

[H_2O/(Al + P) = 10]. Elemental analyses indicate that the occluded organic molecules (TEPA) remain intact after the crystallization processes (see experimental C/N ratios in Table 2).

SAPO34-1 and SAPO34-6 samples, both prepared under very different synthetic conditions and also containing different copper loadings (see Table 2), were selected to study their catalytic behavior on the SCR of NO_x reaction. Those samples show medium-activity (see Fig. 3) when tested with 5% of water in the feed and very high gas hourly space velocity, 450,000 mL/h g_{cat}. However, SAPO34-6, which contains lower Cu-loading in the solid, presents better activities at high temperatures. More interestingly, SAPO34-6 shows similar activity to Cu-exchanged SAPO-34 (see Section 2 for details). Those results clearly indicate the importance of controlling the Cu amount in extra-framework positions into the final solids for the catalytic activity on the SCR of NO_x.

3.2. Direct synthesis of Cu-SAPO-34 using different amounts of Cu-TEPA with an excess of TEPA molecules

As reported above, the large amount of copper-complex required in the synthesis media [Cu-TEPA/(Al + P) = 0.5] to achieve Cu-SAPO-34 materials promotes a very large loading of copper in

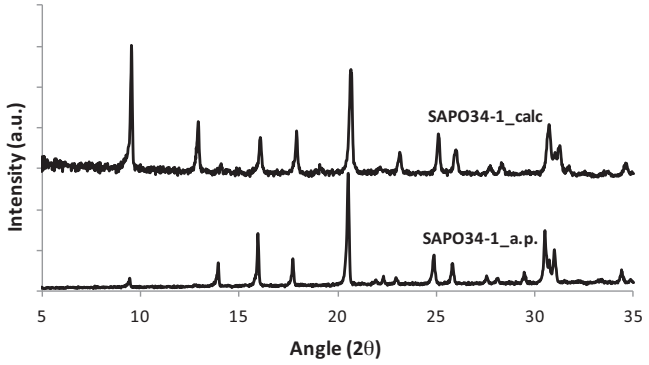

Fig. 2. XRD patterns of Cu-SAPO34-1 in as-prepared and calcined form.

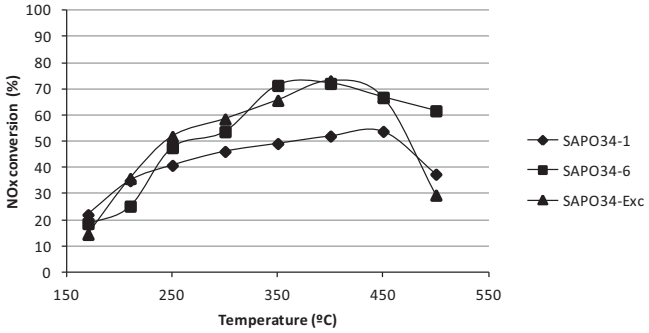

Fig. 3. Catalytic activity for the SCR of NO_x reaction of Cu-SAPO-34 materials synthesized using Cu-TEPA as the unique organic molecule and Cu exchanged SAPO-34.

Table 3
Experimental design for the direct hydrothermal synthesis of silicoaluminophosphates by using controlled amounts of Cu-complex and an excess of TEPA (T = 150 °C static conditions, t = 7 days).

Variable	Values
Cu-TEPA/(Al + P)	0.1, 0.2, 0.3, 0.4
[TEPA/(Al + P)]	[0.4, 0.3, 0.2, 0.1, respectively]
H_2O/(Al + P)	30
P/Al	0.8, 0.9
[Si/(Al + P)]	[0.2, 0.1, respectively]

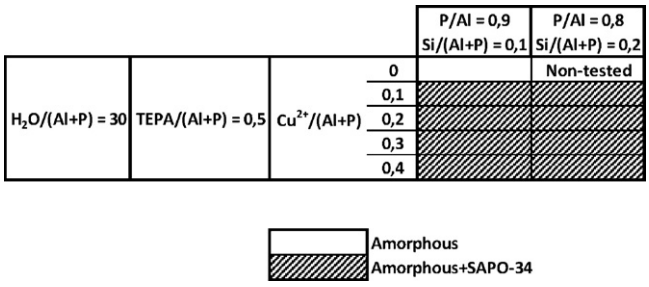

Fig. 4. Phases obtained for the direct hydrothermal synthesis of Cu-SAPO-34 using different amounts of Cu-complex (Cu-TEPA) with the addition of an excess of TEPA.

the final solid [Cu/(Al + P) between 0.13 and 0.21, see Table 2]. If Cu-TEPA complex quantity is reduced from the synthesis gel, only amorphous materials were achieved (see Fig. 1). Therefore, a new strategy must be defined in order to synthesize SAPO-34 materials by direct methodologies but with controlled Cu-loadings. In this sense, we decided to prepare a new set of experiments where defined ratios of Cu-complex were fixed [Cu-TEPA/(P + Al) = 0.1, 0.2, 0.3, 0.4] in combination with an excess of TEPA molecules (see experimental design in Table 3), which would act as co-organic space fillers, and consequently, would permit the diminution of Cu atoms in the final crystalline materials.

Unfortunately, only mixtures of SAPO-34 and amorphous materials were obtained in all experiments when the combination of Cu-TEPA complex and TEPA molecules was used for the direct preparation of Cu-SAPO-34 materials (see Fig. 4). Fig. 5 shows the low crystalline nature of the achieved samples.

3.3. Direct synthesis of Cu-SAPO-34 using different amounts of Cu-TEPA with a cooperative OSDA (diethylamine, DEA)

In order to improve the crystallization of SAPO-34 with reduced and controlled Cu-complex amounts, we decided to study the introduction of a different cooperative OSDA, such as diethylamine (DEA), which is an organic molecule widely used in the preparation of regular SAPO-34 [17]. In this sense, controlled quantities of Cu-complex [Cu-TEPA/(Al + P) = 0.05, 0.1, 0.15 and 0.2] were

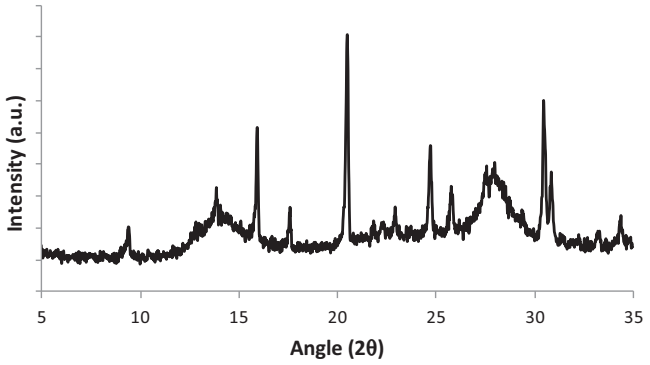

Fig. 5. XRD pattern of the most crystalline material obtained using Cu-TEPA in combination with an excess of TEPA molecules.

Table 4
Experimental design for the direct hydrothermal synthesis of Cu-SAPO-34 using different amounts of Cu-complex (Cu-TEPA) in combination with a cooperative OSDA (diethylamine, DEA) (T = 150 °C static conditions).

Variable	Values
Cu-TEPA/(Al + P)	0.05, 0.1, 0.15, 0.2
[DEA/(Al + P)]	[0.45, 0.4, 0.35, 0.3, respectively]
H_2O/(Al + P)	10
P/Al	0.8, 0.9
[Si/(Al + P)]	[0.2, 0.1, respectively]
Time (days)	1, 7

studied by adding into the mixture an excess of the cooperative organic molecule DEA, keeping constant the total amount of organic molecules [Cu-TEPA/(Al + P) + DEA/(Al + P) = 0.5]. The experimental design is summarized in Table 4.

As seen in Fig. 6, SAPO-34 materials were obtained with different amounts of Cu-complex in the synthesis media, when the Si/(Al + P) ratio was fixed in 0.2, after 7 days at 150 °C. Interestingly, the preparation of fully crystalline SAPO-34 can be remarkably improved when small amounts of SAPO-34 seeds (5 wt% of expected final yield) were introduced in the mixture (see Fig. 6). The XRD patterns of the as-prepared SAPO34-7, -8, and -9, synthesized with different Cu amounts in the synthesis mixture, are listed in Fig. 7.

The characterization of those directly synthesized Cu-SAPO-34 materials by UV–vis spectroscopy confirms the stability of the Cu-complex after the crystallization. UV–vis spectra of the Cu-TEPA complex in solution and the as-prepared Cu-SAPO-34 materials exhibit a strong band at 270 nm, revealing that Cu-TEPA complex is retained intact after crystallization inside the SAPO-34 materials (see Fig. 8). Those occluded Cu-complex molecules lead the presence of cationic copper extra-framework species after organic removal by calcination.

Chemical and elemental analyses were performed on those three Cu-SAPO-34 materials synthesized by the cooperative OSDA

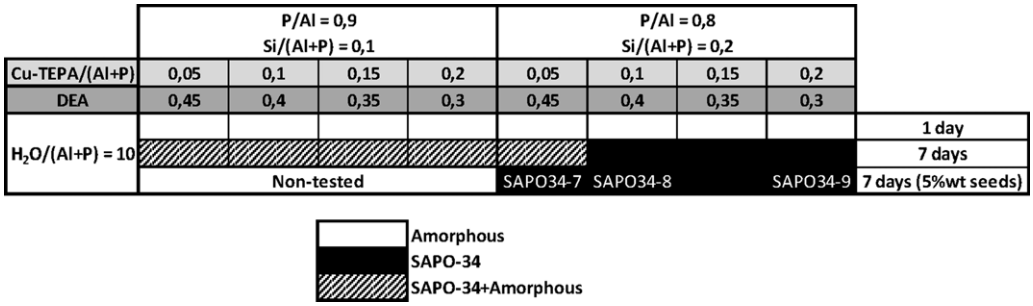

Fig. 6. Phases obtained for the direct hydrothermal synthesis of Cu-SAPO-34 using different amounts of Cu-complex (Cu-TEPA) in combination with a cooperative OSDA (diethylamine, DEA).

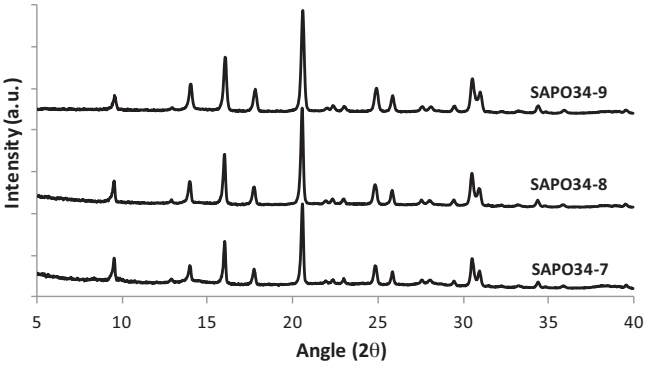

Fig. 7. XRD patterns of the synthesized Cu-SAPO-34 materials using different amounts of Cu-complex (Cu-TEPA) in combination with a cooperative OSDA (diethylamine, DEA).

Table 5
Chemical and elemental analyses of Cu-SAPO-34 samples achieved by using Cu-TEPA and DEA as OSDAs.

Sample	Si/(P + Al)	Cu/(P + Al)	wt% Cu	$(C/N)_{real}$	% DEA	% TEPA
SAPO-7	0.23	0.04	3.4	2.05	20.8	79.2
SAPO-8	0.24	0.07	6.0	1.77	8.3	91.7
SAPO-9	0.22	0.12	10.4	1.73	4.2	95.8

direct methodology (see Table 5). Those analyses demonstrate that different and controlled loading of copper into the final solids is obtained by following the present methodology (see Cu/(P + Al) in Table 5). Moreover, a good correlation between the amount of DEA and TEPA into the final solids is found depending on the initial theoretical ratio of Cu-TEPA (the larger the theoretical Cu-TEPA ratio, the higher the content of TEPA into the final solid), clearly

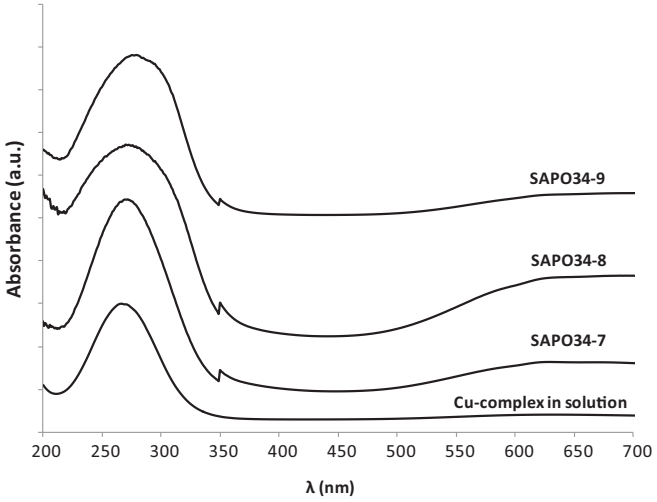

Fig. 8. UV–vis spectra of Cu-TEPA complex in solution, and as-prepared Cu-SAPO-34 materials.

evidencing a controlled insertion of the Cu-complex during the nucleation–crystallization processes.

More importantly, the final solid yields of the Cu-SAPO-34 materials obtained after their calcination are higher than 90%. Those values are much higher than previously reported yields on the direct synthesis of Cu-SAPO-34 provided by researchers at BASF (~70%) [15c].

SEM images of the three directly synthesized Cu-SAPO-34 materials reveal cubic crystals with similar averaged sizes (6–10 μm) (see Fig. 9).

The catalytic activity of those Cu-SAPO-34 materials was studied under severe catalytic conditions (presence of 5% of water in the

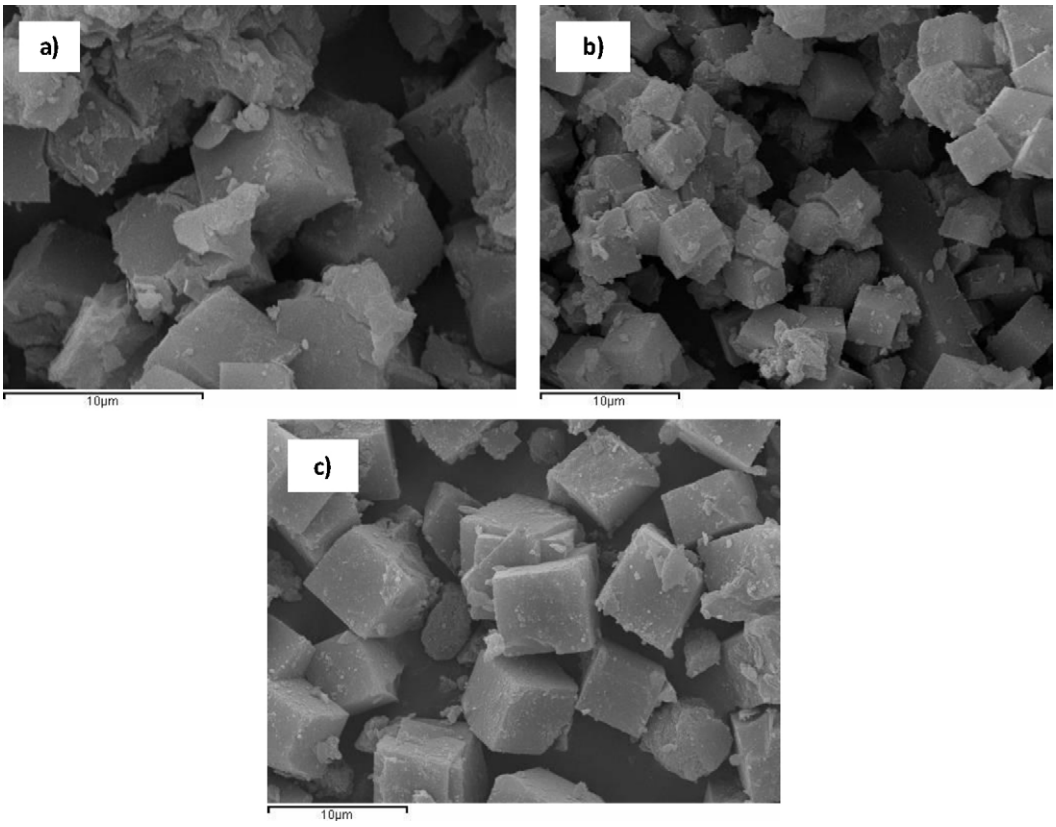

Fig. 9. SEM image of (a) SAPO34-7, (b) SAPO34-8 and (c) SAPO34-9.

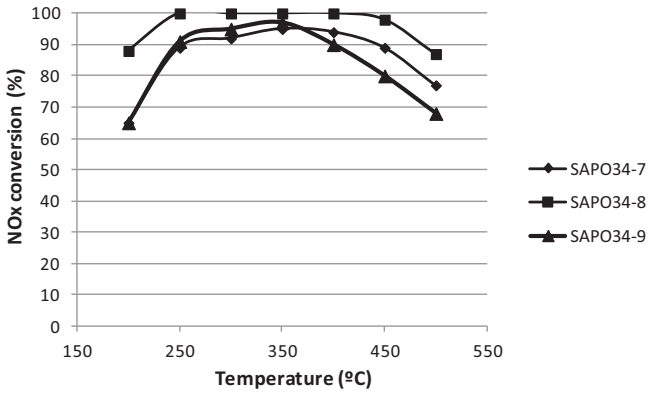

Fig. 10. Catalytic activity for the SCR of NO_x reaction of Cu-SAPO-34 materials synthesized using different amounts of Cu-complex (Cu-TEPA) in combination with a cooperative OSDA (diethylamine, DEA).

feed and very high gas hourly space velocity, 450,000 mL/h g_{cat}). As reported in Fig. 10, those materials proceed very well for the SCR of NO_x. Particularly, SAPO34-8 shows an exceptional catalytic profile, indicating that the intermediate extra-framework Cu-loading [Cu/(Al + P) = 0.07] seems to be the optimum metal charge for those materials. Those catalytic results clearly indicate that SAPO-34 materials, especially SAPO34-8, are very active for SCR of NO_x reaction. At this time, further analysis on the product distribution must be performed in order to study the selectivity of those materials towards the desired N_2 formation.

Additional characterization has been performed on the optimum SAPO34-8 in order to study its microporosity, and the coordination of the atoms present in the support. The N_2 adsorption isotherm at 77 K shown in Fig. 11 reveals the microporous nature of SAPO34-8, with a micropore volume of 0.14 cm^3/g. The coordination of the atoms present in the support was studied by solid-state NMR. ^{31}P MAS NMR indicates a single signal at −28 ppm indicative of one distinguishable type of tetrahedral phosphorous (see Fig. 12A). ^{27}Al MAS NMR spectrum exhibits a strong peak at 35 ppm, which corresponds to Al in tetrahedral environments in the framework [18], while the signal at 10 ppm has been assigned to five-coordinated aluminum in the framework of SAPO-34 with water molecules (see Fig. 12B) [19]. Finally, ^{29}Si MAS NMR spectrum indicates that part of silicon atoms are selectively replacing phosphorous atoms in the framework (see signal at −91 ppm in

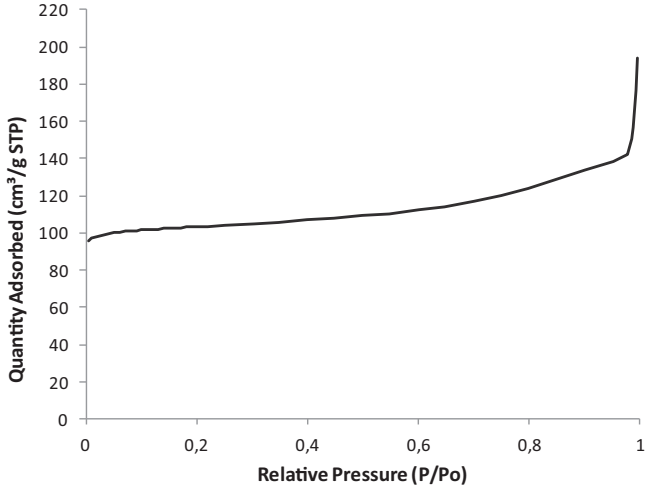

Fig. 11. N_2 adsorption isotherm obtained for SAPO34-8 material.

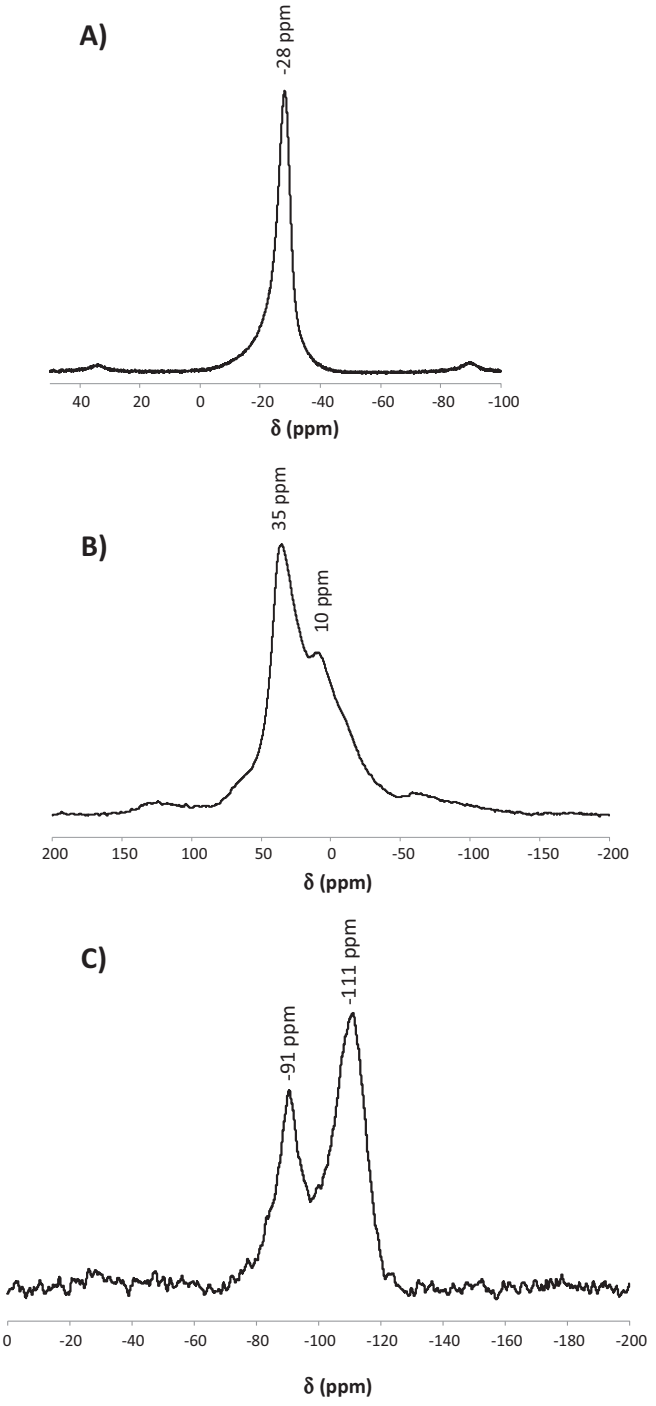

Fig. 12. Solid-state NMR spectra of SAPO34-8: (a) ^{31}P MAS NMR, (b) ^{27}Al MAS NMR, and (c) ^{29}Si MAS NMR.

Fig. 12C), while the signal at −111 ppm reveals that Si-rich domains are also present in the final solid.

3.4. Hydrothermal stability of Cu-SAPO-34 materials synthesized using different amounts of Cu-TEPA with a cooperative OSDA (diethylamine, DEA)

The hydrothermal stability of those three Cu-SAPO-34 materials synthesized using different amounts of Cu-TEPA with a cooperative OSDA were further studied by performing steaming treatments at high temperatures (600 and 750 °C) during 13 h. As shown in Fig. 13, all three samples show excellent hydrothermal stability

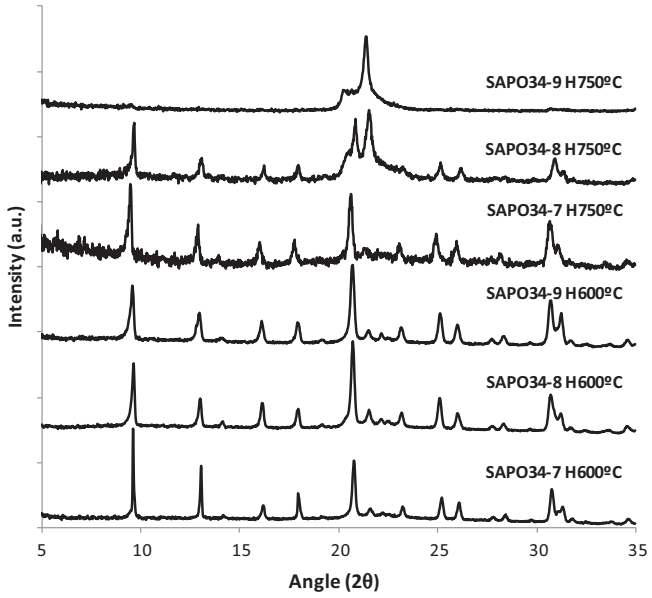

Fig. 13. XRD patterns of Cu-SAPO-34 materials after severe steam treatments.

when treated at 600 °C in presence of steam for long time periods. The catalytic activity for SCR of NO_x was tested for those hydrothermally treated samples, and as seen in Fig. 14, both SAPO34-8 and -9 proceed with conversions higher than 90% in most of the tested temperatures, while SAPO34-7 shows conversion values close to 70%. Despite the similar activity profile between SAPO34-8 and -9, better conversions are achieved at higher temperatures when working with the former, illustrating the enhanced catalytic behavior of the intermediate Cu-loading SAPO-34, even after the steaming treatment.

However, when Cu-SAPO-34 materials were treated under more extreme conditions at 750 °C in presence of steam for 13 h, SAPO34-7 sample shows an excellent hydrothermal stability when compared to the other samples (see Fig. 13). Indeed, it seems that there is a clear correlation between the Cu content and the hydrothermal stability of the Cu-SAPO-34 at 750 °C. In this case, hydrothermally treated SAPO34-7 material was tested on the SCR of NO_x catalyst, obtaining NO_x conversions close to 70% in a very broad temperature profile (see Fig. 14). Those results are very similar to the achieved values on SAPO34-7 when was treated at 600 °C, indicating that Cu environments have not significantly changed after the hydrothermal treatment at 600 or 750 °C.

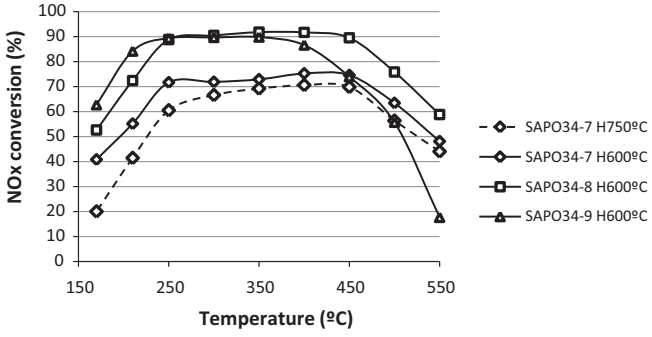

Fig. 14. Catalytic activity for the SCR of NO_x reaction of Cu-SAPO-34 materials synthesized using different amounts of Cu-complex (Cu-TEPA) in combination with a cooperative OSDA (diethylamine, DEA) after steam treatments.

4. Conclusions

The rational use of the Cu-TEPA complex combined with an additional organic molecule (as DEA) allow the inexpensive direct synthesis of Cu-SAPO-34 material with controlled Cu-loading into the final solids, and very high yields of solids after calcination (>90% of the expected solid). The range of Cu-loading into the final solids is much higher than with other previously reported Cu-SAPO-34 materials synthesized by direct methodologies and, importantly, those Cu atoms are primary in extra-framework cationic form (Cu-complex molecule remains unaltered inside of the as-prepared Cu-SAPO-34, as confirmed by UV–vis spectroscopy). Moreover, those materials perform very well in the SCR of NO_x reaction, making those materials and their synthesis methodology very promising for their industrial application.

Acknowledgements

This work has been supported by Haldor-Topsoe, Consolider Ingenio 2010-Multicat, and UPV through PAID-06-11 (no. 1952). MM acknowledges to "Subprograma Ramon y Cajal" for the contract RYC-2011-08972.

References

[1] V.I. Parvulescu, P. Grange, B. Delmon, Catalysis Today 46 (1998) 233–316.
[2] R.M. Heck, R.J. Farrauto, S.T. Gulati, Catalytic Air Pollution Control, Wiley Intersciences, New York, 2002.
[3] (a) P. Forzatti, L. Lietti, Heterogeneous Chemistry Reviews 3 (1996) 33–51;
(b) S. Brandenberger, O. Kröcher, A. Tissler, R. Althoff, Catalysis Reviews – Science and Engineering 50 (2008) 492–531.
[4] E. Jacob, R. Müller, A. Schneeder, T. Cartus, R. Dreisbach, H. Mai, M. Paulus, J. Spengler, Motortechnische Zeitschrift (2006) 67.
[5] (a) R.Q. Long, R.T. Yang, Journal of Catalysis 188 (1999) 332–339;
(b) R.Q. Long, R.T. Yang, Journal of the American Chemical Society 121 (1999) 5595–5596.
[6] M. Iwamoto, H. Furukawa, Y. Mine, F. Uemura, S.I. Mikuriya, S. Kagawa, Journal of the Chemical Society, Chemical Communications (1986) 1272–1273.
[7] (a) B. Modén, P. Da Costa, B. Fonfé, D.K. Lee, E. Iglesia, Journal of Catalysis 209 (2002) 75–86;
(b) M.H. Groothaert, J.A. van Bokhoven, A.A. Battiston, B.M. Weckhuysen, R.A. Schoonhetdt, Journal of the American Chemical Society 125 (2003) 7629–7640;
(c) I. Melian-Cabrera, S. Espinosa, J.C. Groen, B. Van de Liden, F. Kapteijn, J.A. Mouliijn, Journal of Catalysis 238 (2006) 250–259;
(d) A. Corma, V. Fornés, A.E. Palomares, Applied Catalysis B 11 (1997) 233–242;
(e) A. Corma, A. Palomares, F. Marquez, Journal of Catalysis 170 (1997) 132–139.
[8] I. Bull, R.S. Boorse, W.M. Jaglowski, G.S. Koermer, A. Moini, J.A. Patchett, W.M. Xue, P. Burk, J.C. Dettling, M.T. Caudle, U.S. Patent 0,226,545 (2008).
[9] (a) D.W. Fickel, E. D'addio, J.A. Lauterbach, R. Lobo, Appl. Catal. B 102 (2011) 441–448;
(b) J.H. Kwak, R.G. Tonkyn, D.H. Kim, J. Szanyi, C.H.F. Peden, Journal of Catalysis 275 (2010) 187–190;
(c) S.T. Korhonen, D.W. Fickel, R.F. Lobo, B.M. Weckhuysen, A.M. Beale, Chemical Communications 47 (2011) 800–802.
[10] D.W. Fickel, R.F. Lobo, Journal of Physical Chemistry C 114 (2010) 1633–1640.
[11] (a) L. Ren, L. Zhu, C. Yang, Y. Chen, Q. Sun, H. Zhang, C. Li, F. Nawaz, F.-S. Xiao, Chemical Communications 47 (2011) 9789–9791;
(b) L. Ren, Y. Zhang, S. Zeng, L. Zhu, Q. Sun, H. Zhang, C. Yang, X. Meng, X. Yang, F.-S. Xiao, Chinese Journal of Catalysis 33 (2012) 92–105.
[12] S.Y. Chung, S.H. Oh, M.H. Kim, I.S. Nam, Y.G. Kim, Catalysis Today 54 (1999) 521–529.
[13] B.M. Lok, C.A. Messina, R.L. Patton, R.T. Gajek, T.R. Cannan, E.M. Flanigen, Journal of the American Chemical Society 106 (1984) 6092–6093.
[14] (a) T. Ishihara, M. Kagawa, F. Hadama, Y. Takita, Journal of Catalysis 169 (1997) 93–102;
(b) H.-X. Li, W.E. Cormier, B. Moden, US2008/0241060 (2008).;
(c) P.J. Andersen, J.E. Collier, J.L. Casci, H.-Y. Chen, J.M. Fedeyko, R.K.S. Foo, R.R. Rajaram, WO2008/132452 (2008).
[15] (a) B.I. Palella, M. Cadoni, A. Frache, H.O. Pastore, R. Pirone, G. Russo, S. Coluccia, L. Marchese, Journal of Catalysis 217 (2003) 100–106;
(b) A. Frache, M. Cadoni, S. Coluccia, L. Marchese, B. Palella, R. Pirone, P. Ciambelli, Studies in Surface Science and Catalysis 135 (2001) 328;
(c) I. Bull, U. Muller, US2010/0310440A1 (2010).

[16] U. Deka, I. Lezcano-Gonzalez, S.J. Warrender, A. Lorena, P.A. Wright, B.M. Weckhuysen, A.M. Beale, Microporous and Mesoporous Materials (2012), http://dx.doi.org/10.1016/j.micromeso.2012.04.056.
[17] G. Liu, P. Tian, J. Li, D. Zhang, F. Zhou, Z. Liu, Microporous and Mesoporous Materials 111 (2008) 143–149.
[18] A.M. Prakash, S. Unnikrishnan, Journal of the Chemical Society, Faraday Transactions 90 (1994) 2291–2296.
[19] G. Liu, P. Tian, Y. Zhang, J. Li, L. Xu, S. Meng, Z. Liu, Microporous and Mesoporous Materials 114 (2008) 416–423.